Geol. Mag. **155** (*5*), *2018, pp. 1175–1189.* © *Cambridge University Press 2017*
doi:10.1017/S0016756817000085

A Tonian age for the Visingsö Group in Sweden constrained by detrital zircon dating and biochronology: implications for evolutionary events

MAŁGORZATA MOCZYDŁOWSKA*†, VICTORIA PEASE‡, SEBASTIAN WILLMAN*, LINDA WICKSTRÖM§ & HEDA AGIĆ*

*Uppsala University, Department of Earth Sciences, Palaeobiology, Villavägen 16, SE 752 36 Uppsala, Sweden
‡Stockholm University, Department of Geological Sciences, PetroTectonics Facility, Svante Arrhenius väg 8, SE 106 91 Stockholm, Sweden
§Geological Survey of Sweden, Box 670, SE 751 28, Uppsala, Sweden

(*Received* 22 November 2016; *accepted* 30 January 2017; *first published online* 6 March 2017)

Abstract – Detrital zircon U–Pb ages from samples of the Neoproterozoic Visingsö Group, Sweden, yield a maximum depositional age of $\leq 886 \pm 9$ Ma (2σ). A minimum depositional age is established biochronologically using organic-walled and vase-shaped microfossils present in the upper formation of the Visingsö Group; the upper formation correlates with the Kwagunt Formation of the 780–740 Ma Chuar Group in Arizona, USA, and the lower Mount Harper Group, Yukon, Canada, that is older than 740 Ma. Mineralized scale microfossils of the type recorded from the upper Fifteenmile Group, Yukon, Canada, where they occur in a narrow stratigraphic range and are younger than 788 Ma, are recognized for the first time outside Laurentia. The mineralized scale microfossils in the upper formation of the Visingsö Group seem to have a wider stratigraphic range, and are older than *c*. 740 Ma. The inferred age range of mineralized scale microfossils is 788–740 Ma. This time interval coincides with the vase-shaped microfossil range because both microfossil groups co-occur. The combined isotopic and biochronologic ages constrain the Visingsö Group to between $\leq$ 886 and 740 Ma, thus Tonian in age. This is the first robust age determination for the Visingsö Group, which preserves a rich microfossil assemblage of worldwide distribution. The organic and mineralized microorganisms preserved in the Visingsö Group and coeval successions elsewhere document global evolutionary events of auto- and heterotrophic protist radiations that are crucial to the reconstruction of eukaryotic phylogeny based on the fossil record and are useful for the Neoproterozoic chronostratigraphic subdivision.

Keywords: Tonian Visingsö Group, detrital zircon, microfossils, eukaryotic evolution, Baltica

1. Introduction

The tripartite subdivision of the Neoproterozoic Era (ICS Timescale 2015, Cohen *et al*. 2015*a*) reflects the time intervals characterized by global environmental changes related to plate tectonics, climate fluctuations, ocean geochemistry and redox state (Johnston *et al*. 2010; Van Kranendonk *et al*. 2012; Lyons, Reinhard & Planavsky, 2014; Planavsky *et al*. 2015). The radically changing natural environments shaped the ecosystems and stimulated evolutionary modifications of the highest magnitude in the marine realm. The divergence of eukaryotic protists and finally multicellular organisms including animals (Narbonne, 2005; Knoll *et al*. 2006; Porter, 2006; Butterfield, 2011; Knoll, 2014) might have been triggered, along with genetic mutations, by the development of progressively oxygenated marine basins, which existed in warm to temperate climatic zones (Li, Evens & Halverson, 2013; Spence, Le Heron & Fairchild, 2016; Turner & Bekker, 2016). The oxidation of marine basins could have also been influenced by the evolution of increasingly complex eukaryotes (Lenton *et al*. 2014), but also eukaryote evolution could have been more independent of oxygen concentration (Butterfield, 2009; Milles *et al*. 2011; Sperling *et al*. 2013). The oxygen level rose owing to the steady-state photosynthetic production of free oxygen (Falkowski & Raven, 2007; Jackson, 2015; Schirrmeister, Gugger & Donoghue, 2015), and cyanobacteria and red and green algae thrived at the time (Schopf, 1992; Butterfield, 2000; Sergeev, 2006; Moczydłowska, 2008*a*, 2016; Love *et al*. 2009; Moczydłowska *et al*. 2011; Tang *et al*. 2013; Xiao *et al*. 2014*a*,*b*). Oxygen started to accumulate in the atmosphere–hydrosphere system after the Great Oxidation Event (*c*. 2.3 Ga; Holland, 2002; Bekker *et al*. 2004) or possibly earlier (Lyons, Reinhard & Planavsky, 2014; Jackson, 2015; Lalonde & Konhauser, 2015). The ocean redox state fluctuated but oxygen content increased in Neoproterozoic time (Halverson *et al*. 2010; Planavsky *et al*. 2015; Sahoo *et al*. 2016). Although low atmospheric oxygen concentrations might have prevailed during mid Proterozoic time (Lyons, Reinhard & Planavsky, 2014; Planavsky *et al*.

†Author for correspondence: malgo.vidal@pal.uu.se

2014; Li *et al*. 2015), oxygen concentrations might have been higher (Cox *et al*. 2016; Mukherjee & Large, 2016; Tang *et al*. 2016; Zhang *et al*. 2016), including a ventilated or relatively well-oxygenated surface ocean with oxygen oases or oxygen whiffs (Anbar *et al*. 2007; Kaufman, Corsetti & Varni, 2007; Poulton & Canfield, 2011; Partin *et al*. 2013) possibly allowing the deep ocean to remain anoxic and sulfidic (Canfield, 1998; Anbar & Knoll, 2002).

During the Tonian Period (1000 – *c*. 720 Ma), the supercontinent Rodinia was fragmented and rifted along newly formed continental margins creating seaways with active circulation, mixing water masses and increased input of mineral nutrients from the weathering of continental crust (Halverson *et al.* 2010; Li, Evens & Halverson, 2013; Spence, Le Heron & Fairchild, 2016). The subsequent collapse of many ecosystems during the Cryogenian Period (*c*. 720–635 Ma) due to severe ice ages (Hoffman & Schrag, 2002; Eyles & Januszczak, 2007; Allen & Etienne, 2008; Arnaud, Halverson & Shields-Zhou, 2011) caused the extinction of the majority of biotas (Knoll, 1994; Vidal, 1994; Vidal & Moczydłowska-Vidal, 1997). However, this extinction process or reduction in diversity might have been initiated before the onset of the Sturtian glaciation, thus in late Tonian time, due to eutrophication (Nagy *et al*. 2009) or other as yet unclear factors (Riedman *et al*. 2014). Despite the catastrophic Cryogenian environmental conditions, some lineages and discrete cyanobacterial and algal taxa survived the ice ages and even in the meantime originated (*Papillomembrana*), as well as ciliates and foraminifera, during the interglacial cycle(s), as evident from the fossil record in the pre-, inter- and post-Cryogenian successions (Corsetti, Awramik & Pierce, 2003; Moczydłowska 2008*a*,*b*; Nagy *et al*. 2009; Bosak *et al*. 2011, 2012; Riedman *et al*. 2014; Cohen *et al*. 2015*b*; Corsetti, 2015; Ye *et al*. 2015). The recovery of ecosystems following de-glaciation and sea-level rise in the Ediacaran Period (635–541 Ma) paved the way for the exponential radiation of phytoplankton, the rise of multicellular organisms of the Ediacara-type and the bilaterian animals of modern phyla (Grey, 2005, 2007; Narbonne, 2005; Moczydłowska & Nagovitsin, 2012; Narbonne, Xiao & Shields, 2012; Liu *et al*. 2014; Xiao *et al*. 2014*b*).

The environmental and evolutionary history of the Tonian Period is renowned for the development of marine habitats that sustained robust planktonic and benthic communities, and induced further life expansion as is shown by the high diversification of auto- and heterotrophic protists (Vidal & Moczydłowska-Vidal, 1997; Knoll *et al*. 2006; Porter, 2006; Sergeev, 2006; Cohen & Knoll, 2012; Cohen & Macdonald, 2015). However, several microfossil taxa (*Pterospermopsimorpha*, *Valeria*, *Tasmanites, Schizofusa*; certain *Leiosphaeridia*) have persisted since the Mesoproterozoic Era (Yan & Liu, 1993; Lamb *et al*. 2009; Moczydłowska *et al*. 2011; Agić, Moczydłowska & Yin, 2015). The Tonian diversification is well recorded in the Visingsö Group of the Lake Vättern Basin (Fig. 1) and in numerous successions worldwide, such as the Vadsø, Tanafjord and Hedmark groups in Norway, and successions in Russia (the southern Urals and Siberia), the USA (the Chuar Group in Arizona, Uinta Mount Group in Utah and the Pahrump Group in California) and Canada (the Fifteenmile and Harper groups in Yukon) (Vidal, 1976; Vidal & Ford, 1985; Jankauskas, Mikhailova & German, 1989; Horodyski, 1993; Vidal & Moczydłowska, 1995; Porter, 2006; Nagy *et al*. 2009; Cohen & Knoll, 2012; Strauss *et al*. 2014; Porter & Riedman, 2016). The Visingsö Group contains a diverse assemblage of cyanobacteria, stromatolites, organic-walled microfossils (OWM) and vase-shaped microfossils (VSM) (Vidal, 1972, 1976; Martí Mus & Moczydłowska, 2000; Agić, Moczydłowska & Willman, 2015; Loron, 2016). In addition, newly recovered mineralized scale microfossils (MSM; Fig. 2a, b, d; ongoing study) resemble the type known from the Tonian Fifteenmile Group in Yukon, Canada (former Tindir Group; Allison & Hilgert, 1986; Macdonald *et al*. 2011; Cohen & Knoll, 2012).

Until now, the age of the Visingsö Group was estimated palaeontologically to between 800 and 700 Ma (Vidal & Moczydłowska, 1995). Our dating of detrital zircons provides a maximum depositional age of *c*. 886 Ma and, together with the biochronology of common microfossil taxa established in the Chuar and Mount Harper groups at a minimum age of *c*. 740 Ma (Dehler *et al*. 2005; Nagy *et al*. 2009; Strauss *et al*. 2014), is consistent with a Tonian age for the Visingsö Group.

The implications of the Visingsö microfossil record set within a geochronologic framework are significant for reconstructing Neoproterozoic evolutionary events and ecological processes. These are the origin and divergence of phytoplanktonic (many OWM) and heterotrophic (VSM) protists, MSM of uncertain but likely algal affinity (Cohen *et al*. 2011) and benthic bacteria forming microbial mats and stromatolites. Their passive dispersal (cysts of algal phytoplankton and heterotrophs) or active migration (motile vegetative cells of phytoplankton and motile heterotrophic protists) in the marine realm was facilitated by the global hydrological cycle and patterns of current circulation changing at given time intervals throughout the Neoproterozoic period.

2. Geological setting

The Mesoproterozoic Sveconorwegian belt exposed in southwestern Scandinavia (Fig. 1a) represents deeply eroded continental crust reworked during Sveconorwegian (1.14–0.90 Ga) orogenesis (Möller *et al*. 2015 and references therein). The latter is associated with the construction of Rodinia (Pease *et al*. 2008; Bingen, Belousova & Griffin, 2011). Post-orogenic relaxation and gravitational collapse led to uplift and cooling at *c*. 900 Ma (Viola *et al.* 2011). Scandinavia, as part of Baltica, gradually rifted from Rodinia between

https://doi.org/10.1017/S0016756817000085 Published online by Cambridge University Press

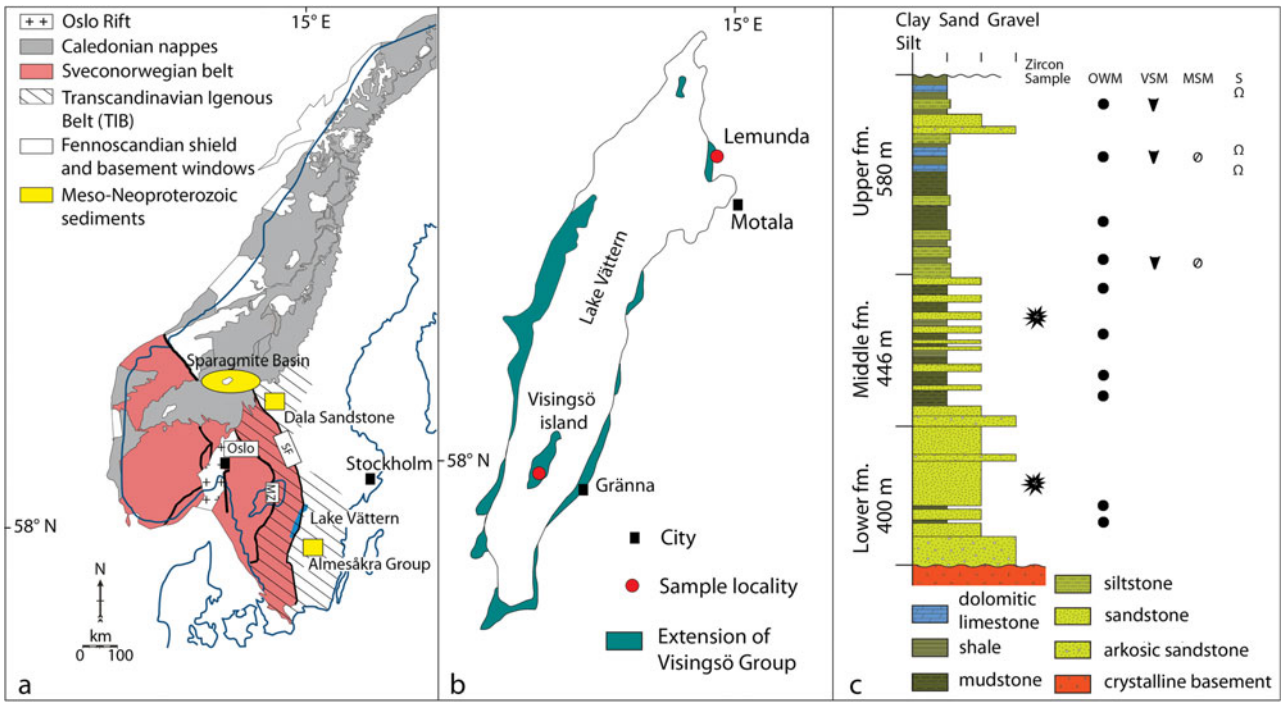

Figure 1. (a) Map of Baltoscandia showing tectonostratigraphic domains of the Caledonides and the Fennoscandian Shield basement with the distribution of the remnant Proterozoic sediments. (b) Extension of the Visingsö Group along Lake Vättern. (c) Lithologic succession with position of studied samples and distribution of microfossils. Modified from Vidal (1982) and Lundmark & Lamminen (2016). Abbreviations: SF – Sveconorwegian deformation front; MZ – Mylonite Zone; OWM – organic-walled microfossils; VSM – vase-shaped microfossils; MSM – mineralized scale microfossils; S – stromatolites; fm. – formation.

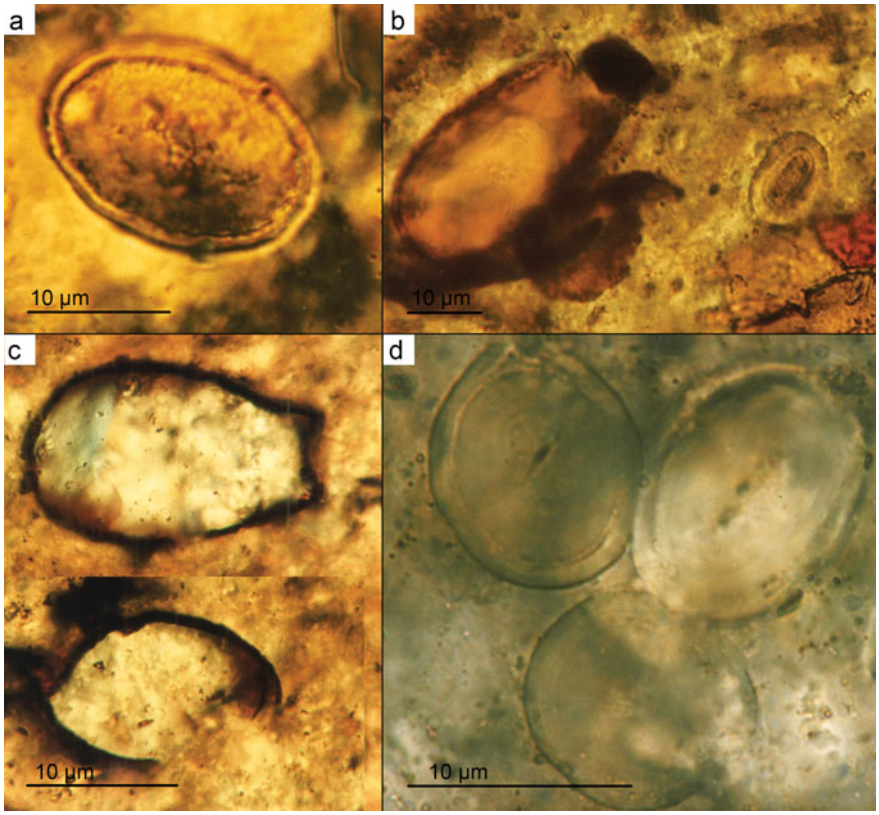

Figure 2. New record of vase-shaped microfossils (b, c) and newly discovered mineralized scale microfossils (a, b, d) preserved in phosphatic nodules in the upper formation of the Visingsö Group. (a) *Paleomegasquama arctoa*, Slide 6, K-35-2. (b) *Cycliocyrillium torquata* (specimen on left side), and *Bicorniculum brochum* (specimen on right side), Slide 6, V40-3. (c) *Melanocyrillium hexadiadema* (upper specimen), Slide 7, M10-4. (d) *Archeoxybaphon polykeramoides*, Slide 7, J24-2. Scale bar equal to 15 μm in (a), 30 μm in (b), 50 μm in (c), 20 μm in (d). Collection PMU-V72G14, Slides 6–7. England Finder Coordinates provided for each specimen.

https://doi.org/10.1017/S0016756817000085 Published online by Cambridge University Press

c. 850 and 630 Ma with concomitant marine transgression (Li, Evens & Halverson, 2013). This paper focuses on the Tonian (1000 – *c*. 720 Ma) depositional history of Fennoscandia.

During Sveconorwegian orogenesis, southeastward imbrication and displacement of the crust occurred. The eastern limit of the orogen is defined by the Sveconorwegian deformation front (SF), a steeply dipping zone of high strain that marks the limit of Sveconorwegian ductile deformation and metamorphism (Möller *et al*. 2015; Fig. 1a). To the east of the SF, igneous and metamorphic rocks of the 2.0–1.75 Ga Svecokarelian orogen and 1.86–1.66 Ga plutonic and volcanic rocks of the Transcandinavian Igneous Belt (TIB) are unaffected by Sveconorwegian ductile deformation or metamorphism (Stephens *et al*. 2009). The orogen-parallel 0.97–0.95 Ga Blekinge-Dalarna dolerite dyke swarm intrudes along and east of the SF (Söderlund *et al*. 2005) and documents the last known magmatic activity along the SF. The SF is a long-lived crustal-scale feature. It was active as early as *c*. 1200 Ma during the early phase of Sveconorwegian orogenesis, and was reactivated later (*c*. 950 Ma) during uplift of the Eastern Segment (e.g. Viola *et al*. 2011). This was followed by the formation of the 'proto-Vättern graben' with deposition of the Visingsö Group in Neoproterozoic time (Vidal & Moczydłowska, 1995).

Late to post-Sveconorwegian sediments are not preserved within the Sveconorwegian belt. Post-orogenic sediments interpreted to reflect rift- and passive-margin settings associated with the break-up of Rodinia were deposited in the Sveconorwegian hinterland (Pease *et al*. 2008). These are now preserved within the nappes (Hedmark Group) and parautochthonous successions (Vadsø and Tanafjord groups) of the Caledonian orogen (Bingen, Belousova & Griffin, 2011). Along the SF, erosional remnants of these sediments, e.g. the Visingsö Group, the Amesåkra Group, the Dala Sandstone and successions in the Sparagmite Basin, unconformably overlie TIB granitoid basement (Bingen, Belousova & Griffin, 2011; Lundmark & Lamminen, 2016; Fig. 1a, b).

3. Visingsö Group succession, previous work and sampling

The Visingsö Group is exposed along Lake Vättern and on Visingsö Island. The Group consists of terrigenous clastic rocks with minor carbonates deposited on TIB-related rocks of various ages (Vidal, 1974, 1976, 1982, 1985; Larson & Nørgaard-Pedersen, 1988; Ulmius, Andersson & Möller, 2015; Fig. 1b). The succession is also known from 15 boreholes penetrating various portions of the strata. The Visingsö strata are unmetamorphosed and undeformed except for local normal faults with low dips of 5–25° (Vidal, 1976; Morad & Al-Aasm, 1994). The Visingsö Group is *c*. 1426 m thick and comprises lower, middle and upper formations (informal nomenclature; Fig. 1c). The lower formation consists of quartzofeldspathic sandstone interbedded with shale and arkosic sandstone (over 400 m in thickness), and represents a progradational fluvial-deltaic environment. The boundary between the lower and middle formations is gradational from quartzitic sandstone coarsening into feldspathic sandstone, respectively. The middle formation comprises feldspathic sandstone and conglomerate succeeded by alternating sandstone, mudstone and shale (at least 446 m), deposited in a pro-delta setting characterized by occasional delta lobes prograding into shallow marine environments. The boundary with the upper formation is sharp at the top of quartz sandstone (middle formation) and the base of laminated mudstone (upper formation). The upper formation consists of alternating shale, mudstone and fine-grained sandstone, and dolomitic limestone with stromatolites (580 m thick). Deposition occurred in a shallow marine, tidally influenced mud flat environment with distinct intervals of subtidal and intertidal sedimentation.

Geological relationships indicate that the Visingsö Group sediments are younger than *c*. 946 Ma, the age of dolerite dykes that cut the granitoid basement upon which the Group is deposited (Söderlund *et al*. 2005). Earlier isotopic studies of the Visingsö Group include K–Ar detrital mica ages (1060–985 Ma; Magnusson, 1960) and Rb–Sr ages on clay and whole-rock fractions of shale from the upper formation (703–663 Ma; Bonhomme & Welin, 1983), ages now interpreted to reflect the time of crystallization and diagenesis, respectively.

We examine three samples from the Visingsö Group at Lake Vättern (Fig. 1b). The lower formation sample (V15-Lem) was collected from the NE wall at the entrance to the Lemunda Quarry, and consists of white-yellowish, medium-grained, weakly consolidated quartz arenite with faint thin bedding. Two samples of the middle formation were collected from the Visingsö 1 borehole on Visingsö Island (Fig. 1b) at depths of 137.50–140.10 m (V15-10) and 120.40–120.95 m (V15-9). They are medium-grained quartzofeldspathic sandstone.

4. Age and provenance of the Visingsö Group from detrital zircons

4.a. Analytical methods

Zircons were separated from 1–2 kg of sample using conventional water table and heavy liquid mineral separation techniques. Approximately 200 zircon grains with various morphologies, sizes and colours were hand-picked onto double-sided tape, cast into epoxy resin, sectioned and polished. A deliberate effort was made to select all zircon colours, sizes, morphologies, etc., during picking. Scanning electron microscope (SEM) and cathodoluminescence (CL) images of the zircons were used to identify textures and select analytical locations; these were obtained

https://doi.org/10.1017/S0016756817000085 Published online by Cambridge University Press

using a FEI SEM at the Department of Geological Sciences, Stockholm University. Analytical methods follow those described in Zhang, Roberts & Pease (2015). Further details of the analytical method are provided in the online Supplementary Material available at http://journals.cambridge.org/geo.

4.b. Analytical results

Our analytical results are summarized below and in Figure 4. The data and inverse concordia diagrams, as well as a more detailed discussion of sediment provenance, are also presented in the online Supplementary Material available at http://journals.cambridge.org/geo (Table S2, and Figures S1, S2 and S3). Errors are reported at the 2-sigma level. For zircon ages younger than 1.2 Ga the ^{206}Pb–^{238}U ages were used in the final analysis and for ages older than 1.2 Ga the ^{207}Pb–^{206}Pb ages were used in the final analysis. Analyses with high common Pb as well as those with > 10 % discordance or > 10 % uncertainties were excluded from the final data synthesis. Concordia diagrams and probability density distribution plots were made using ISOPLOT/Ex 4.15 (Ludwig, 2012).

V15-Lemunda. The lower formation of the Visingsö Group. Zircon from this quartz arenite reflects a diverse detrital assemblage of grains, i.e. aspect ratios of 1:1 to 1:5, a variety of colours, with and without inclusions, and a range of CL textures from igneous oscillatory zoning to uniformly bleached zones indicating secondary fluid migration. The grains are generally low in U (500 ppm or lower in 93 % of the crystals) with diverse Th/U ratios (0.14–2.1). Seventy per cent of the analyses meet the quality assessment criteria (117/154), yielding a continuous spread of ages from 1850–887 Ma (online Supplementary Material available at http://journals.cambridge.org/geo, Fig. S1). Neoproterozoic peaks at *c*. 1026, 945 and 900 Ma dominate the age spectra, while lesser peaks occur at *c*. 1600, 1446, 1268 and 1100 Ma (peak ages typically ± 25 Ma). A weighted mean of the youngest four analyses = 886 ± 9 Ma (MSWD = 0.81, Prob = 0.49) and provides a conservative maximum age for the sediment.

V15-10. The middle formation of the Visingsö Group. Zircon from this quartz-arkosic sandstone, similar to V15-Lem, reflects a diverse detrital assemblage of grains with the addition of CL-dark rim overgrowths on most grains. The grains have moderate U concentrations with 77 % between 100 and 700 ppm, 13 % < 100 ppm and 10 % > 1000 ppm. Modern lead-loss is apparent in the $^{238}U/^{206}Pb$ versus $^{207}Pb/^{206}Pb$ concordia diagram, in accord with high-U grains and metamictization. Th/U ratios are diverse (0.08–2.4). Sixty per cent of the analyses meet the quality assessment criteria (98/165), yielding a continuous spread of ages from 1913–990 Ma (online Supplementary Material available at http://journals.cambridge.org/geo, Fig. S2). Palaeoproterozoic to Mesoproterozoic peaks dominate the age spectra, namely *c*. 1751, 1625 and 1450 Ma, while a spread of ages occurs at *c*. 1300–990 Ma with a minor peak at *c*. 992 Ma. A weighted mean of the youngest three analyses = 997 ± 13 Ma (MSWD = 0.38, Prob = 0.68) and provides the maximum age of the sediment.

V15-9. The middle formation of the Visingsö Group. Zircon from this quartz-arkosic sandstone also reflects a diverse detrital assemblage of grains with the addition of CL-dark rim overgrowths on most grains. The grains range from 32–1152 ppm U, with 71 % between 100 and 500 ppm, and 5 % > 1000 ppm. Modern lead-loss is also apparent in the $^{238}U/^{206}Pb$ versus $^{207}Pb/^{206}Pb$ concordia diagram. Th/U ratios are diverse (0.04–3.6). Seventy-five per cent of the analyses meet the quality assessment criteria (132/168) and yield a continuous spread of ages from 1878–1043 Ma (online Supplementary Material available at http://journals.cambridge.org/geo, Fig. S3). The dominant peaks in the detrital spectra are Mesoproterozoic in age, namely *c*. 1640, 1580 and 1439 Ma, while older (*c*. 1780 Ma) and younger ages (*c*. 1260–1045 Ma) are minor contributors to the age spectra. A weighted mean of the two youngest analyses = 1050 ± 15 Ma (MSWD = 0.57, Prob = 0.45) and provides a maximum age for the sediment.

Our new LA-ICP-MS U–Pb detrital zircon data from the three Visingsö samples provide maximum depositional ages for the middle formation of ≤ 1050 ± 15 Ma (2σ; V15-9) and ≤ 997 ± 13 Ma (2σ; V15-10), and for the lower formation of ≤ 886 ± 9 Ma (2σ; V15-Lem) (Fig. 4). The youngest age, obtained from the lower formation, represents the best estimate of the maximum depositional age for the Visingsö Group at *c*. 886 Ma.

4.c. Provenance

The provenance of the Visingsö zircons is consistent with derivation from the igneous, metamorphic and recycled sedimentary rocks known to be exposed in the region at the time of deposition, i.e. Svecokarelian rocks (*c*. 2.0–1.75 Ga), TIB (*c*. 1.86–1.66 Ga plutonic and volcanic rocks), metamorphic and igneous rocks associated with the Gothian (1.66–1.52 Ga), Hallandian (*c*. 1.47–1.38 Ga) and Sveconorwegian (*c*. 1.14–0.90 Ga) orogens (Möller *et al.* 2015; Lundmark & Lamminen, 2016), as well as swarms of 1.6–0.95 Ga dolerite dykes (Söderlund *et al.* 2005) that intrude the Fennoscandian basement. In addition, the Meso- to Neoproterozoic sediments now only locally preserved across the shield (e.g. Morad & Al-Aasm, 1994; Bingen, Belousova & Griffin, 2011; Lundmark & Lamminen, 2016; Fig. 1a), sources within the Sveconorwegian belt that include a far-travelled Laurentian component and sources from Fennoscandia east of the belt (Bingen, Belousova & Griffin, 2011) are also potential contributors. Thus, we regard the Visingsö Group as predominantly regionally derived. That the stratigraphically lowest sample contains the youngest zircons suggests either (i) increasingly older rocks

https://doi.org/10.1017/S0016756817000085 Published online by Cambridge University Press

were being unroofed and eroded, or (ii) an expanding depositional system covered younger, more locally derived material with older, more distal material. We are unable to distinguish between these two scenarios.

5. Age of the Visingsö Group from diagnostic assemblages

An approximate relative age of *c*. 800–700 Ma for the Visingsö Group has been previously inferred by correlating diagnostic assemblages of OWM, VSM and stromatolites with successions that have an established chronostratigraphy (Vidal & Moczydłowska, 1995; Martí Mus & Moczydłowska, 2000). Such assemblages are known from the Hedmark, Vadsø and Tanafjord groups in the Caledonides of Norway, the Thule and Eleonore Bay groups of Greenland, the Chuar, Uinta Mountain and Pahrump groups in the western USA, the Little Dal, Mount Harper and Fifteenmile groups in Canada, and others in Siberia, the Urals and Svalbard (Vidal, 1976; Vidal & Ford, 1985; Horodyski, 1993; Vidal & Moczydłowska-Vidal, 1997; Porter & Knoll, 2000; Porter, 2006; Nagy *et al*. 2009; Strauss *et al.* 2014). Recent datings of the successions in the western USA and Canada provide more accurate age constraints (Strauss *et al*. 2014). The VSM and certain OWM taxa in the upper formation of the Visingsö Group (Figs 2, 3; list of species in the online Supplementary Material available at http://journals.cambridge.org/geo), which co-occur in the Kwagunt Formation (the upper Chuar Group) and the Callison Lake dolostone (informal unit in the lower Mount Harper Group), provide a biochronological minimum age for the Visingsö Group of *c*. 740 Ma (see Section 6 discussion below). Thus, the Visingsö Group is now robustly constrained to < 886–740 Ma.

6. Discussion and evolutionary implications

The Tonian Visingsö Group documents a diverse microbial association of prokaryotic cyanobacteria and eukaryotic OWM, VSM (Vidal, 1972, 1976; Martí Mus & Moczydłowska, 2000; Agić, Moczydłowska & Willman, 2015; Loron, 2016) and new MSM that are partly identified. The MSM could represent biomineralizing green algae (Cohen *et al*. 2011; Cohen & Knoll, 2012) adding another dimension to the complex ecosystem and development of biomineralization. A new record of OWM, including *Cerebrosphaera*, *Valeria*, *Schizofusa*, *Simia*, *Tasmanites* and *Pterospermopsimorpha* among other taxa (Fig. 3; online Supplementary Material available at http://journals.cambridge.org/geo), strengthen the ranges of potential species for Neoproterozoic biostratigraphy. These taxa are recognized as possible members of green algal lineages of Prasinophyceae and Chlorophyceae (Grey, 2005; Lamb *et al*. 2009; Moczydłowska *et al*. 2011; Moczydłowska, 2016; Agić, Moczydłowska & Willman, 2015; Loron, 2016), but many other OWM taxa remain unidentified phylogenetically. Geochronologically better understood, and now constrained by isotopic dating, the Visingsö microbiota will contribute to reconstructing the relationships among early eukaryotes (Knoll, 2014) by further reconciling the fossil record with molecular clock estimates.

The recognition and identification of OWM, VSM and MSM microfossils allows us to make biochronologic correlations with the Chuar, lower Mount Harper and the upper Fifteenmile groups. The Visingsö microfossils, both uni- and multicellular, are well preserved, abundant and consist of established as well as new species. Some have features that support their various protistan affinities (ongoing study). The OWM in the Visingsö Group were originally described by Vidal (1976) from all formations and additional records derive from the middle and upper formations (Agić, Moczydłowska & Willman, 2015; Loron, 2016; ongoing study; Fig. 3; online Supplementary Material available at http://journals.cambridge.org/geo). The assemblage consists of 20 species recognized by distinct morphology (surface sculpture, excystment structure, wall perforation) and bodyplan (sphere-in-sphere, internal body). Several new species, including those with spinous ornamentation, await formal description. A great variety of spheroidal specimens displaying a wide range of vesicle size and wall thickness, which are attributed by some authors to different species of *Leiosphaeridia* (*crassa*, *jacutica*, *minutissima* and *tenuissima*), are left under open nomenclature as *Leiosphaeridia* spp. Their quantity is enormous (thousands of specimens), yet they lack objective morphologic features and overlap in dimensions to make identification reliable. The cyanobacterial coccoidal and filamentous microfossils preserved as solitary specimens, colonies and fragmentary bacterial mats are attributed to seven genera with more numerous species. In total, the OWM record is among the highest diversity recognized in a single Tonian-age stratigraphic unit. This diversity is of the same taxonomic magnitude as in the Chuar Group assemblage accounting for some 32 OWM species (Nagy *et al*. 2009; Porter & Riedman, 2016), and many are in common. Thus, we correlate the middle and upper formations of the Visingsö Group with the Chuar Group. The lower formation of the Visingsö Group consists of spheroidal and cyanobacterial species that are not age-diagnostic.

The VSM in the upper formation of the Visingsö Group are recorded in unmetamorphosed phosphate nodules embedded in organic-rich mudstone and shale (Knoll & Vidal, 1980; Martí Mus & Moczydłowska, 2000; unpub. data). The phosphate nodules are composed of francolite, a cryptocrystalline phosphate. These were precipitated early in diagenesis in suboxic to sulfate-reduction zones within decimetres to metres of burial below the sediment–water interface (Morad & Al-Aasm, 1994) on tidal mud flats (Larson & Nørgaard-Pedersen, 1988). Francolite precipitation was microbially mediated and microbial mats

https://doi.org/10.1017/S0016756817000085 Published online by Cambridge University Press

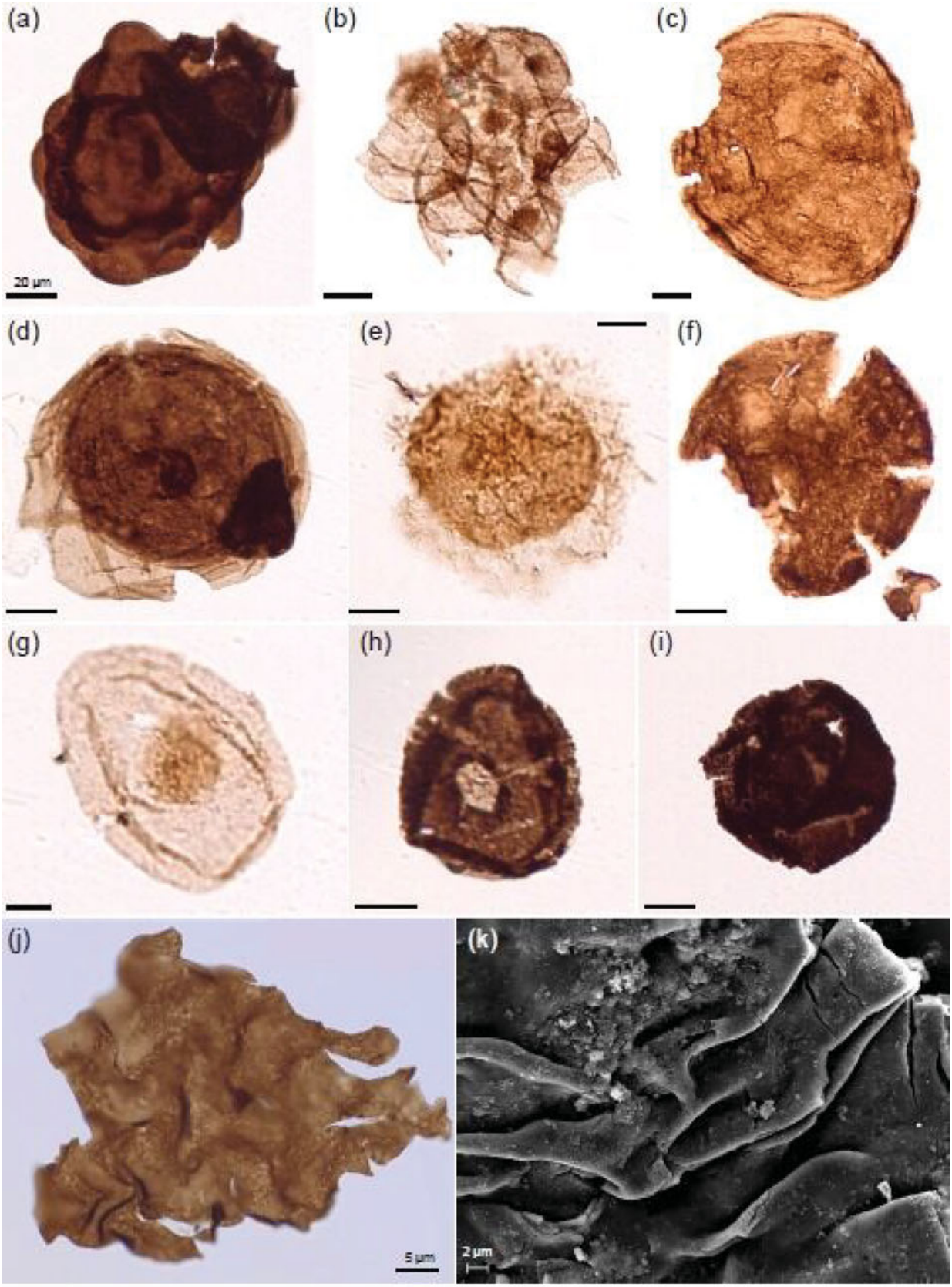

Figure 3. New record of organic-walled microfossils from the upper formation of the Visingsö Group, (a–i) light transmitted and (j, k) scanning electron micrographs. (a) *Squamosphaera colonialica,* V14-66-4-(J44). (b) *Synsphaeridium* sp., V14-14-3-(F30-3). (c) *Valeria lophostriata*, V14-14-3-(J28). (d) *Simia annulare*, V14-14-3-(P24-4). (e) *Pterospermopsimorpha pileiformis*, V14-79-4-(M37-4). (f) *Leiosphaeridia ternata*, V14-14-3-(L25-3). (g) *Leiosphaeridia* sp., V14-36-5-(S44). (h, i) *Lanulatisphaera laufeldii*, V14-66-4-(C40-3); V14-66-4-(U39-1). (j, k) *Cerebrosphaera globosa* (Ogurtsova & Sergeev, 1989) Sergeev & Schopf, 2010; (j) V14-80-4-L57; (k) V14-52-1-04. Scale bars equal 20 μm for light transmitted micrographs. Collection PMU-Visingsö.2014 (V14- followed by the sample and slide numbers, and England Finder Coordinates).

https://doi.org/10.1017/S0016756817000085 Published online by Cambridge University Press

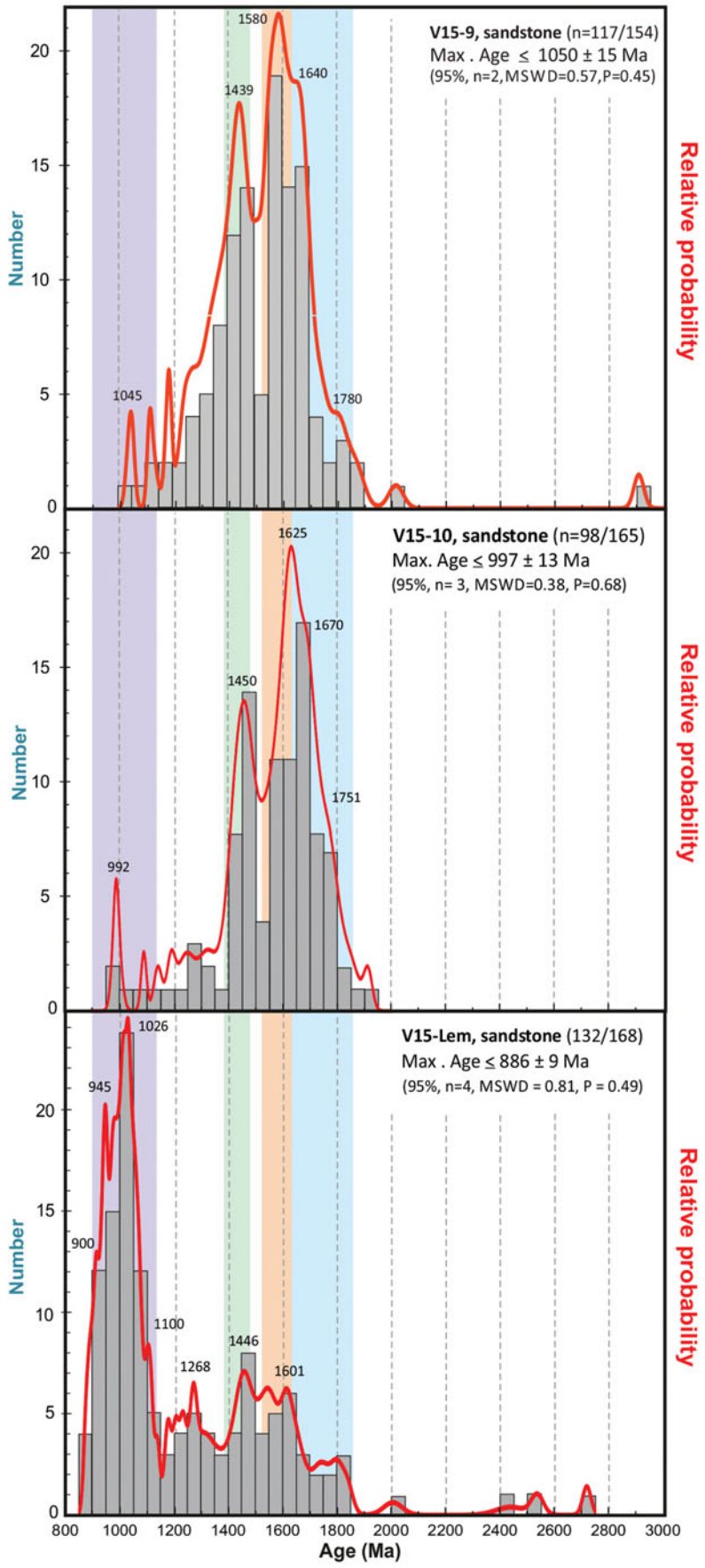

Figure 4. Probability density distribution plots of detrital zircons and their ages from the Visingsö Group sandstones in stratigraphic order. The Sveconorwegian (0.90–1.14 Ga), Hallandian (1.38–1.47 Ga), Gothian (1.52-1.66 Ga) and TIB (1.66–1.86 Ga) sources are indicated (grey bars).

https://doi.org/10.1017/S0016756817000085 Published online by Cambridge University Press

occur as patches and thin discontinuous laminae in the nodules and host mudstone. VSM are abundant, with up to several hundred specimens present in a single petrographic thin-section, and mostly observed in longitudinal or slightly transversal sections. No perpendicular-to-the-long-axis sections or sections through the oral part of the tests are seen in thin-section.

The VSM preserved as three-dimensional organic-walled tests and extracted by acid maceration are known only from the Eleonore Bay Group of East Greenland (Vidal, 1979), the Kwagunt Formation of the Chuar Group type locality (Bloeser, 1985; Porter & Knoll, 2000; Porter, Meinsterfeld & Knoll, 2003) and from the Tien Shan Mountains in Kyrgyzstan (Jankauskas, Mikhailova & German, 1989). Mostly they are preserved as permineralized casts and moulds (Martí Mus & Moczydłowska, 2000; Porter & Knoll, 2000; Porter, Meinsterfeld & Knoll, 2003; Strauss *et al*. 2014). The Visingsö specimens have not yet been isolated from the rock matrix or nodules, and are observed as casts and moulds replicated by precipitation of francolite, quartz and berthierine (Martí Mus & Moczydłowska, 2000). Therefore, their identification is limited to the overall habit and symmetry of the tests observed in thin-section without oral opening ornamentation and shape. We identified *Melanocyrillium hexadiadema* Bloeser, 1985 (Fig. 2c, upper specimen) by distinguishing in a longitudinal section test flexure marking the oral termination (neck-like region) and an invaginated aperture between broad indentation, though the transversal section of the hexagonal aperture was not seen. Synonymy, based on comparable thin-sections of the species, includes specimens illustrated by Bloeser (1985, fig. 7:14; identical to our specimens), Porter, Meinsterfeld & Knoll (2003, fig. 4:11) and Strauss *et al*. (2014, fig. 2A). A specimen with an apertural margin with a minimal short collar and flushing into the test wall (Fig. 2b) is similar to a thin-section illustration by Porter, Meinsterfeld & Knoll (2003, fig. 6:21) and attributed to *Cycliocyrillium torquata* Porter, Meisterfeld & Knoll, 2003. The species is also recognized in the assemblage studied by Martí Mus & Moczydłowska (2000, fig. 3A; see Porter, Meinsterfeld & Knoll, 2003), alongside *Cycliocyrillium simplex* Porter, Meisterfeld & Knoll, 2003 (Martí Mus & Moczydłowska, 2000, figs 6A, C–F, 7A–C, E–F). The latter species is recognized by a bulbous outline of the test with a simple aperture that is relatively narrow in relation to the test width and without any marginal thickening, as seen in the SEM image and the thin-section illustration by Porter, Meinsterfeld & Knoll (2003, fig. 6:9). These authors also suggested this species might be present in the Visingsö assemblage studied by Knoll & Vidal (1980, fig. 1D–G), as well as *Trigonocyrillium horodyski* (Bloeser, 1985) Porter, Meinsterfeld & Knoll, 2003 and *T. fimbriatum* (Bloeser, 1985) Porter, Meinsterfeld & Knoll, 2003, although the two latter species were without reference to individual specimens or collection. *T. fimbriatum* has been documented only by SEM images in the type collection (Bloeser, 1985), but an elongate test with oral fringe seen in the longitudinal view (Bloeser, 1985, figs 10:2_1, 4_1, 7_1, 11:3) is very similar to the specimen illustrated by Martí Mus & Moczydłowska (2000, fig. 2D). This makes a record of five common geographically distributed VSM species in the upper formation of the Visingsö Group among 12 species known in total from the upper Kwagunt Formation (Porter & Knoll, 2000; Porter, Meinsterfeld & Knoll, 2003). Three species (*M. hexadiadema*, *C. simplex* and *C. torquata*) also co-occur in the assemblage of eight species recorded in the Callison Lake dolostone of the lower Mount Harper Group, Yukon, Canada (Strauss *et al*. 2014). Allison & Awramik (1989) reported an older stratigraphic record of VSM in this area (the Tindir Creek, Yukon) from the upper Tindir Group (now the upper Fifteenmile Group; Macdonald *et al*. 2010*a*,*b*, 2011; Cohen & Knoll, 2012) that underlies the Callison Lake dolostone and additionally some 670 m thick succession belonging to the Craggy Dolostone Formation. They document VSM *Melanocyrillium* sp. and new species *Hyalocyrillium clardyi* Allison *in* Allison & Awramik, 1989, along with MSM. The latter taxon was recognized by Allison & Awramik (1989) as being similar to VSM from the Visingsö Group (and successions in Greenland, Brazil and Saudi Arabia) but differing from those in the Chuar Group described by Bloeser (1985) by having a thicker wall. This morphologic or taphonomic difference is insignificant and *H. clardyi* belongs to the VSM, thus proving the co-occurrence of VSM with MSM (Allison & Awramik, 1989; Cohen & Knoll, 2012).

The new genus and species *Hyalocyrillium clardyi* (Allison & Awramik, 1989, fig. 10:10–11) is similar if not identical to *Cycliocyrillium simplex* (Porter, Meinsterfeld & Knoll, 2003, thin-section fig. 6:9) and the two taxa are considered conspecific. This synonymy implies that *Hyalocyrillium* Allison *in* Allison & Awramik, 1989 has taxonomic priority over *Cycliocyrillium* Porter, Meinsterfeld & Knoll, 2003, and its type species *C. simplex* is a junior synonym of the type species *H. clardyi*. Consequently, we recommend that *C. torquata* Porter, Meinsterfeld & Knoll, 2003 should be transferred to *H. torquata* (Porter, Meinsterfeld & Knoll, 2003) new combination, although we do not formalize it in this paper.

The range of VSM in Laurentia was recognized within the time interval *c*. 780–740 Ma (Dehler, 2014; Strauss *et al*. 2014) and, as aforementioned, they extend through a number of formations across the western margin of Laurentia from the Grand Canyon to the Yukon Territory. In the Yukon, the range of VSM through the Callison Lake dolomite (Strauss *et al*. 2014) is in fact wider and extends into the upper Fifteenmile Group to above the isotopically dated layer at 811.5 Ma (Allison & Awramik, 1989; Macdonald *et al*. 2010*b*; Cohen & Knoll, 2012). This poses the need to (i) correlate the upper Fifteenmile Group with other successions containing VSM, and (ii) extend the VSM

https://doi.org/10.1017/S0016756817000085 Published online by Cambridge University Press

lower range to *c*. 788 Ma, consistent with the MSM range (see below).

MSM occur side-by-side with VSM (Fig. 2b) in the upper formation of the Visingsö Group at two stratigraphic levels (Fig. 1c) and they are of the type of scale-like microfossils known from the 811.5–739.9 Ma upper Fifteenmile Group of the Yukon Territory, Canada (Allison & Hilgert, 1986; Macdonald *et al*. 2010*a*,*b*, 2011; Cohen *et al*. 2011; Cohen & Knoll, 2012; Strauss *et al*. 2014). Their discovery in the Visingsö succession for the first time documents their occurrence outside the type locality on Laurentia and is significant because their stratigraphic range is wider than previously recorded. This is evident from their vertical distribution within a rock succession of shale and mudstone *c*. 300 m thick (Fig. 1c) in comparison to the interval of 58 m of limestone containing MSM in the upper Fifteenmile Group (Cohen & Knoll, 2012). Regardless of the different rates of sedimentation between the fine-grained siliciclastic versus carbonate rocks in the two localities, both accumulating in shallow subtidal environments (Larson & Nørgaard-Pedersen, 1988; Macdonald *et al*. 2011, respectively), it appears that the MSM vertical range in the Visingsö Group involves a longer time span.

The Visingsö MSM are observed in thin-sections of phosphate nodules in shale and have not yet been successfully isolated from the host rock to see their three-dimensional morphology, thus making the identification preliminary. They are simple morphotypes, ellipsoidal in outline, smooth in appearance and not perforated, with sharply defined narrow marginal rims and central portion (Fig. 2a, b) or showing additionally one or two marks or holes in the centre (Fig. 2d). Their dimensions are 18–39 μm in length, with 1.5–6.0 μm wide marginal rims. The present specimens, by comparison with specimens observed in thin-sections of chert nodules but also with those isolated from the Fifteenmile Group limestone, are identified as *Paleomegasquama arctoa* Cohen & Knoll, 2012 (Fig. 2a), *Bicorniculum brochum* Allison & Hilgert, 1986 (Fig. 2b) and *Archeoxybaphon polykeramoides* (Allison & Hilgert, 1986) emend. Cohen & Knoll, 2012 (Fig. 2d). The specimen of *P. arctoa* (Fig. 2a) is an ellipsoidal scale, 21 × 30 μm in diameter, with a smooth surface and two distinct portions: a narrow marginal rim 1.5–2.3 μm in width and a large central portion. It resembles isolated Fifteenmile Group specimens of placolith form and is of their dimensions (Cohen & Knoll, 2012, fig. 9.7–9.9), and if seen in section it would be identical to the specimen illustrated by Cohen & Knoll (2012, in fig. 9.8). The specimen of *B. brochum* (Fig. 2b) is an ellipsoidal scale, 30 × 39 μm in diameter, with two marginal rings: a narrow inner and a wider outer, together 6 μm in width, around a central ellipsoidal portion. It is similar to specimens in illustrated thin-sections by Allison & Hilgert (1986, figs 10.1, 10.2), although the tooth-like band is not visible clearly in our section. However, the higher dimensional proportion of the two rings to the small central portions of the scale is typical of the species and differs from other scale microfossils. The species *A. polykeramoides* is an elliptical scale, 18 × 25 μm in diameter, smooth without any visible pores, with a thin marginal rim and 1–2 central elongate markings or holes. Certain three-dimensionally preserved Fifteenmile Group specimens show elevated elements or holes in the central portion of the scale (Cohen & Knoll, 2012, figs 3.1, 3.5), which if sectioned would appear similar to those in the Visingsö specimens (Fig. 2d).

The stratigraphic position of MSM in the type area of the Western Ogilvie Mountains, Yukon, in the Lower Tindir Group, upper shale informal unit, has been defined to be above the Bitter Springs C-isotopic anomaly stage, which is also recognized in the upper Fifteenmile Group in the Central Ogilvie Mountains above the horizon isotopically dated to 811.5 Ma (Macdonald *et al*. 2010*b*). The MSM described in detail by Cohen & Knoll (2012) have been subsequently attributed to the upper Fifteenmile Group, and tentatively to its Craggy Dolomite Formation in the Mt Slipper section, where the fossiliferous strata are 58 m thick. This is the same lithostratigraphic unit as the 'limestone unit of the upper Tindir Group' in the Tindir Creek locality studied originally by Allison & Hilgert (1986).

Uncertainty remains regarding the lithostratigraphic attribution of MSM, because of recent re-mapping and re-assessment of rock successions in the Yukon Territory, and revision of their stratigraphic position and regional correlation based on isotopic dating and δ^{13}C chemostratigraphy (Macdonald *et al*. 2010*a*,*b*, 2011; Macdonald & Roots, 2010; Strauss *et al*. 2014). The chronostratigraphy of these units has also changed and although previously attributed to the Cryogenian (850–635 Ma) is now referred to the Tonian Period (1000 – *c*. 720 Ma), following the International Chronostratigraphic Chart 2015 (Cohen *et al*. 2015*a*).

The stratigraphic position of MSM, whether in the basal Craggy Dolostone or at the top of the Reefal Assemblage, is constrained by the age of the Bitter Springs Stage (BSS). The BSS has been recognized as a globally synchronous C-isotope negative anomaly (Halverson *et al*. 2010) and is constrained to the interval after 811.5 Ma and before 788.7 Ma, lasting *c*. 7–17 Ma (Macdonald *et al*. 2010*b*; Swanson-Hysell *et al*. 2015). MSM occur above the BSS, thus their maximum age is *c*. 788 Ma. The range of MSM in the Ogilvie Mountains type area is very short and equal to the depositional time of 58 m thick limestone that may be just a few million years calculated from the rate of deposition of the succession (*c*. 1000 m thick carbonate succession deposited within the time interval 811–740 Ma). A wider vertical range that is closer to the minimum age of MSM is recorded in the Visingsö Group.

MSM in the upper formation of the Visingsö Group co-occur with more diverse VSM taxa known from the upper Kwagunt Formation and the Callison Lake dolostone (including *M. hexadiadema*) and are understood

https://doi.org/10.1017/S0016756817000085 Published online by Cambridge University Press

to record their upper stratigraphic range and minimum age. This is inferred from the present correlation of the upper formation of the Visingsö Group with these formations and constrained by the minimum age at 740 Ma of the Callison Lake dolostone (Strauss *et al*. 2014). The MSM lower range and maximum age is recognized in the upper Fifteenmile Group and it coincides also with the earliest occurrence of VSM. The MSM upper range and minimum age are recorded in the upper formation of the Visingsö Group together with those of the VSM and indicates the time span of both microfossil groups at *c*. 788–740 Ma.

Tonian marine ecosystems were dominated, as seen in the fossil record by their taxonomic diversity and relative abundance (Porter, 2006; Nagy *et al*. 2009; Cohen & Macdonald, 2015; Tang *et al*. 2015), and enhanced by the new record from the Visingsö Group (represented by thousands of specimens; unpub. data), by photosynthesizing cyanobacteria and algae, and less frequently occurring heterotrophic protists, and some protists of uncertain origin (Butterfield, 2000; Porter, 2006; Sergeev, 2006; Cohen & Macfadden 2015; Porter & Riedman, 2016). Shallow marine habitats must have been relatively well oxygenated to sustain planktonic and benthic autotrophs, allowing them to fulfil their metabolic and life cycle requirements for sexual reproduction, as known from modern analogues (see discussion by Moczydłowska, 2008*a*, 2016). Relatively well-oxygenated ocean surface waters or at least oxygenated local basins in such a state are supported by geochemical studies (Jackson, 2015; Lalonde & Konhauser, 2015; Turner & Bekker, 2016; Spence, Le Heron & Fairchild, 2016) and this is in agreement with the presence of a microbiota of inferred algal affinities that were reproducing sexually in the Visingsö Group at the time, and in contemporaneous successions. Progressive evolution of phytoplankton in the Tonian Period, evident by comparison with the Mesoproterozoic record (Yan & Liu, 1993; Javaux, Knoll & Walter, 2004; Lamb *et al*. 2009; Agić, Moczydłowska & Yin, 2015; Sergeev *et al*. 2016), contributed to steady oxygenation of surface waters by the release of free oxygen, increased the production of net organic matter at the base of the food web and supported heterotrophic consumers – all related to the process of photosynthesis. The integrated environmental and evolutionary development with a positive feedback in a sustainable biosphere is first observed in the Tonian Period.

7. Conclusions

A Tonian age for the Visingsö Group is well defined by combining the maximum age of deposition from U–Pb dating of detrital zircons with the minimum age from biochronologic correlation of the Visingsö Group with the Chuar and the lower Mount Harper groups. This restricts its age to $\leq$ 886–740 Ma, and furthermore restricts its middle and upper formations to *c*. 788–740 Ma. These ages can be extrapolated to successions containing similar assemblages in the Caledonides, Greenland, southern Urals and elsewhere.

We report the presence of a diverse assemblage of OWM and several species of VSM, as well as the recovery of MSM similar to those from the Tonian upper Fifteenmile Group, Yukon, Canada, and for the first time outside Laurentia. We infer the time range of VSM and MSM at *c*. 788–740 Ma, which is constrained by isotopic datings of strata recording their lowermost and uppermost co-occurrence.

Geochronological constraint on the Visingsö microfossil assemblage is significant for revealing the time sequence of evolutionary events and divergence of auto- and heterotrophic protist lineages and for tracing their passive dispersal and active migration between the palaeocontinents. The presence of cosmopolitan taxa indicates a free connection with a global ocean and circulation of surface currents allowing biotic expansion along contiguous continental margins.

The evolution of marine ecosystems comprising similar biotas during the Tonian Period along newly opening marine basins on the margins of Baltica (Visingsö, Hedmark, Vadsø, Tanafjord and Barents Sea successions) and Laurentia (Chuar, Uinta Mountain, Pahrump, Little Dal, Mount Harper and Fifteenmile successions) established the first truly global and diverse eukaryotic protistan biosphere.

Acknowledgements. Our research was supported by Swedish Research Council (Vetenskåpsrådet) project grants Nr 621-2012-1669 to MM and Nr 621-2014-4375 to VP. The Geological Survey of Sweden (SGU) is kindly acknowledged for the access to the Visingsö 1 drillcore. The work of LW was conducted with the kind permission of the SGU Director. We thank the reviewers, Kathleen Grey and one anonymous reviewer, and the editor Mark Allen for their useful comments on the manuscript and the editorial work.

Supplementary material

To view supplementary material for this article, please visit https://doi.org/10.1017/S0016756817000085.

References

Agić, H., Moczydłowska, M. & Yin, L.-M. 2015. Affinity, life cycle, and intracellular complexity of organic-walled microfossils from the Mesoproterozoic of Shanxi, China. *Journal of Paleontology* **89**, 28–50.

Agić, H., Moczydłowska, M. & Willman, S. 2015. Prasinophyte world: biodiversity of organic-walled microfossils from the Cryogenian Visingsö Group, Sweden. In *2015 Geological Society of America Annual Meeting, 2015 Baltimore, Maryland, USA*, *Abstracts. Geological Society of America Abstracts with Programs* **47** (7), 143.

Allen, P. A. & Etienne, J. L. 2008. Sedimentary challenge to Snowball Earth. *Nature Geosciences* **1**, 817–25.

Allison, C. W. & Awramik, S. M. 1989. Organic-walled microfossils from earliest Cambrian or latest Proterozoic Tindir Group Rocks, northwest Canada. *Precambrian Research* **43**, 253–94.

Allison, C. W. & Hilgert, J. W. 1986. Scale microfossils from the Early Cambrian of northwest Canada. *Journal of Paleontology* **60**, 973–1015.

Anbar, A. D., Duan, Y., Lyons, T. W., Arnold, G. L., Kendall, B., Creaser, R. A., Kaufman, A. J., Gordon, G. W., Scott, C., Garvin, J. & Buick, R. 2007. A whiff of oxygen before the Great Oxidation Event? *Science* **317**, 1903–6.

Anbar, A. D. & Knoll, A. H. 2002. Proterozoic ocean chemistry and evolution: a bioinorganic bridge. *Science* **297**, 1137–42.

Arnaud, E., Halverson, G.P. & Shields-Zhou, G. (eds). 2011. *The Geological Record of Neoproterozoic Glaciations*. Geological Society of London, Memoir no. 36, 735 pp.

Bekker, A., Holland, H. D., Wang, P.-L., Rumble III, D., Stein, H. J., Hannah, J. L., Coetzee, L. L. & Beukes, N. J. 2004. Dating the rise of atmospheric oxygen. *Nature* **427**, 117–20.

Bingen, B., Belousova, E. A. & Griffin, W. L. 2011. Neoproterozoic recycling of the Sveconorwegian orogenic belt: detrital-zircon data from the Sparagmite basins in the Sveconorwegian Caledonides. *Precambrian Research* **189**, 347–67.

Bloeser, B. 1985. *Melanocyrillium*, a new genus of structurally complex Late Proterozoic microfossils from the Kwagunt Formation (Chuar Group), Grand Canyon, Arizona. *Journal of Paleontology* **59**, 41–765.

Bonhomme, M. G. & Welin, E. 1983. Rb–Sr and K–Ar isotopic data on shale and siltstone from the Visingsö Group, Lake Vättern basin, Sweden. *Geologiska Föreningens i Stockholm Förhandlingar* **105**, 363–6.

Bosak, T., Lahr, D. J. G., Pruss, S. B., Macdonald, F. A., Gooday, A. J., Dalton, L. & Matys, E. 2012. Possible early foraminiferans in post-Sturtian (716–635 Ma) cap carbonates. *Geology* **40**, 67–70.

Bosak, T., Macdonald, F., Lahr, D. & Matys, E. 2011. Putative Cryogenian ciliates from Mongolia. *Geology* **39**, 1123–6.

Butterfield, N. J. 2000. *Bangiomorpha pubescens* n. gen.: implications for the evolution of sex, multicellularity, and the Mesoproterozoic/Neoproterozoic radiation of euakaryotes. *Paleobiology* **26**, 386–404.

Butterfield, N. J. 2009. Oxygen, animals, and oceanic ventilation: an alternative view. *Geobiology* **7**, 1–7.

Butterfield, N. J. 2011. Animals and the invention of the Phanerozoic Earth system. *Trends in Ecological and Evolution* **26**, 81–7.

Canfield, D. E. 1998. A new model for Proterozoic ocean chemistry. *Nature* **396**, 450–53.

Cohen, K. M., Finney, S. C., Gibbard, P. L. & Fan, J.-X. 2015a. The ICS International Chronostratigraphic Chart, v2015/01. http://www.stratigraphy.org/ICSchart/ChronostratChart2015-01.pdf.

Cohen, P. A. & Knoll, A. H. 2012. Scale microfossils from the mid-Neoproterozoic Fifteenmile Group, Yukon Territory. *Journal of Paleontology* **86**, 775–800.

Cohen, P. A. & Macdonald, F. A. 2015. The Proterozoic record of Eukaryotes. *Paleobiology* **41**, 610–32.

Cohen, P. A., Macdonald, F. A., Pruss, S., Matys, E. & Bosak, T. 2015b. Fossils of putative marine algae from the Cryogenian glacial interlude of Mongolia. *Palaios* **30**, 238–47.

Cohen, P. A., Schopf, J. W., Butterfield, N. J., Kudryavtsev, A. B. & Macdonald, F. A. 2011. Phosphate biomineralization in mid-Neoproterozoic protists. *Geology* **39**, 539–42.

Corsetti, F. A. 2015. Life during Neoproterozoic Snowball Earth. *Geology* **43**, 559–60.

Corsetti, F. A., Awramik, S. M. & Pierce, D. 2003. A complex microbiota from Snowball Earth times: microfossils from the Neoproterozoic Kingston Peak Formation, Death Valley, USA. *Proceedings of the National Academy of Sciences USA* **100**, 4399–404.

Cox, G. M., Jarrett, A., Edwards, D., Crockford, P. W., Halverson, G., Collins, A. S., Poirier, A. & Li, Z.-X. 2016. Basin redox and primary productivity within the Mesoproterozoic Roper Seaway. *Chemical Geology* **440**, 101–14.

Dehler, C. M. 2014. Advances in Neoproterozoic biostratigraphy spark new correlations and insight in evolution of life. *Geology* **42**, 731–2.

Dehler, C. M., Elrick, M., Bloch, J. D., Crossey, L. J., Karstrom, K. E. & Des Marais, D. J. 2005. High-resolution $\partial^{13}C$ stratigraphy of the Chuar Group (ca. 770–742 Ma), Grand Canyon: implications for mid-Proterozoic climate change. *Geological Society of America Bulletin* **117**, 32–45.

Eyles, N. & Januszczak, N. 2007. "Zipper-rift": a tectonic model for Neoproterozoic glaciations during the breakup of Rodinia after 750 Ma. *Earth-Science Reviews* **65**, 1–73.

Falkowski, P. G. & Raven, J. A. 2007. *Aquatic Photosynthesis*. Princeton and Oxford: Princeton University Press, 484 pp.

Grey, K. 2005. Ediacaran palynology of Australia. *Association of Australasian Palaeontologists Memoir* **31**, 1–439.

Grey, K. 2007. The world of the very small: fueling the Animalia. In *The Rise of Animals Evolution and Diversification of the Kingdom Animalia* (eds M. A. Fedonkin, J. G. Gehling, K. Grey, G. M. Narbonne & P. Vickers-Rich), pp. 219–31. Baltimore: The Johns Hopkins University Press.

Halverson, G. P., Wade, B. P., Hurtgen, M. T. & Barovich, K. M. 2010. Neoproterozoic chemostratigraphy. *Precambrian Research* **182**, 337–50.

Hoffman, P. F. & Schrag, D. P. 2002. The Snowball Earth hypothesis: testing the limits of global change. *Terra Nova* **14**, 129–55.

Holland, H. 2002. Volcanic gases, black smokers, and the Great Oxidation Event. *Geochimica et Cosmochimica Acta* **66**, 3811–26.

Horodyski, R. J. 1993. Paleontology of Proterozoic shales and mudstones: examples from the Belt Supergroup, Chuar Group and Pahrump Group, western USA. *Precambrian Research* **61**, 241–78.

Jackson, T. A. 2015. Variations in the abundance of photosynthetic oxygen through Precambrian and Paleozoic time in relation to biotic evolution and mass extinctions: evidence from Mn/Fe ratios. *Precambrian Research* **264**, 30–5.

Jankauskas, T. V., Mikhailova, N. S. & German, T. N. (eds). 1989. *Microfossili Dokembriya SSSR (Precambrian Microfossils of the USSR)*. Trudy Instituta Geologii i Geochronologii Dokembrya SSSR. Leningrad: Akademia Nauk, 188 pp. (in Russian).

Javaux, E., Knoll, A. H. & Walter, M. R. 2004. TEM evidence for eukaryotic diversity in mid-Proterozoic oceans. *Geobiology* **2**, 121–32.

Johnston, D. T., Poulton, S. W., Dehler, C., Porter, S., Husson, J., Canfield, D. E. & Knoll, A. H. 2010. An emerging picture of Neoproterozoic ocean chemistry: insights from the Chuar Group, Grand Canyon, USA. *Earth and Planetary Science Letters* **290**, 64–73.

Kaufman, A. J., Corsetti, F. A. & Varni, M. A. 2007. The effect of rising atmospheric oxygen on carbon and sulfur isotope anomalies in the Neoproterozoic Johnnie Formation, Death Valley, USA. *Chemical Geology* **237**, 47–63.

Knoll, A. H. 1994. Proterozoic and Early Cambrian protists: evidence for accelerating evolutionary tempo. *Proceedings of the National Academy of Sciences USA* **91**, 6743–50.

Knoll, A. H. 2014. Paleobiological perspectives on early eukaryotic evolution. *Cold Spring Harbor Perspectives in Biology* **6**, a016121, 14 pp. doi: 10.1101/cshperspect.a016121.

Knoll, A. H., Javaux, E. J., Hewitt, D. & Cohen, P. 2006. Eukaryotic organisms in Proterozoic oceans. *Philosophical Transactions of the Royal Society London, Series B* **361**, 1023–38.

Knoll, A. H. & Vidal, G. 1980. Late Proterozoic vase-shaped microfossils from the Visingsö Beds, Sweden. *Geologiska Föreningen i Stockholm Förhandlingar* **102**, 2017–211.

Lalonde, S. V. & Konhauser, K. O. 2015. Benthic perspective on Earth's oldest evidence for oxygenic photosynthesis. *Proceedings of the National Academy of Sciences USA* **112**, 995–1000.

Lamb, D. M., Awramik, S. M., Chapman, D. J. & Zhu, S. 2009. Evidence for eukaryotic diversification in the ∼1800 million-year-old Changzhougou Formation, North China. *Precambrian Research* **173**, 93–104.

Larsen, M. & Nørgaard-Pedersen, N. 1988. *A Sedimentological Analysis of Deltaic Complexes and Alluvial Fan Deposits in the Visingsö Group (Upper Proterozoic), Southern Sweden*, Vol. l. Institut for Almen Geologi Københavns Universitet, 199 pp.

Lenton, T. M., Boyle, R. A., Poulton, S. W., Shields-Zhou, G. A. & Butterfield, N. J. 2014. Co-evolution of eukaryotes and ocean oxygenation in the Neoproterozoic Era. *Nature Geoscience* **7**, 257–65.

Li, Z.-X., Evens, D. A. D. & Halverson, G. P. 2013. Neoproterozoic glaciations in a revised global palaeogeography from the breakup of Rodinia to the assembly of Gondwanaland. *Sedimentary Geology* **294**, 219–32.

Li, C., Planavsky, N. J., Love, G. D., Reinhard, C. T., Hardisty, D., Feng, L., Bates, S. M., Huang, J., Zhang, Q., Chu, X. & Lyons, T.W. 2015. Marine redox conditions in the middle Proterozoic ocean and isotopic constraints on authigenic carbonate formation: insights from the Chuanlinggou Formation, Yanshan Basin, North China. *Geochimica et Cosmochimica Acta* **150**, 90–105.

Liu, P., Xiao, S., Yin, C., Chen, S., Zhou, C. & Li, M. 2014. Ediacaran acanthomorphic acritarchs and other microfossils from chert nodules of the Upper Doushantuo Formation in the Yangtze Gorges area, South China. *Journal of Paleontology* **88**, 1–139.

Loron, C. 2016. *The biodiversity of organic-walled eukaryotic microfossils from the Tonian Visingsö Group, Sweden*. M.Sc. thesis, Department of Earth Sciences, Uppsala University, Uppsala, Sweden. Nr 366, 103 pp. Published thesis.

Love, G. D., Grosjean, E., Stalvies, C., Fike, D. A., Grotzinger, J. P., Bradley, A. S., Kelly, A. E., Bhatia, M., Meredith, W., Snape, C. E., Bowring, S. A., Condon, D. J. & Summons, R. E. 2009. Fossil steroids record the appearance of Demospongiae during the Cryogenian period. *Nature* **457**, 718–21.

Ludwig, K. 2012. *Isoplot/Ex Version 3.75, A Geochronological Toolkit for Microsoft Excel*. Berkeley Geochronology Center Special Publication no. 5, pp. 75.

Lundmark, A. M. & Lamminen, J. 2016. The provenance and setting of the Mesoproterozoic Dala Sandstone, western Sweden, and paleogeographic implications for southwestern Fennoscandia. *Precambrian Research* **275**, 197–208.

Lyons, T. W., Reinhard, C. T. & Planavsky, N. J. 2014. The rise of oxygen in Earth's early ocean and atmosphere. *Nature* **506**, 307–15.

Macdonald, F. A., Cohen, P. A., Dudás, F. Ö. & Schrag, D. P. 2010a. Early Neoproterozoic scale microfossils in the Lower Tindir Group of Alaska and the Yukon territory. *Geology* **38**, 143–6.

Macdonald, F. A. & Roots, C. F. 2010. Upper Fifteenmile Group in the Ogilvie Mountains and correlations of early Neoproterozoic strata in the northern Cordillera. In *Yukon Exploration and Geology 2009* (eds K. E. MacFarlane, L. H. Weston & L. R. Blackburn), pp. 237–52. Yukon Geological Survey.

Macdonald, F. A., Schmitz, M. D., Crowley, J. L., Roots, C. F., Jones, D. S., Maloof, A. C., Strauss, J. V., Cohen, P. A., Johnston, D. T. & Schrag, D. P. 2010b. Calibrating the Cryogenian. *Science* **327**, 1241–3.

Macdonald, F. A., Smith, E. F., Strauss, J. V., Cox, G. M., Halverson, G. P. & Roots, C. F. 2011. Neoproterozoic and early Paleozoic correlations in the western Ogilvie Mountains, Yukon. In *Yukon Exploration and Geology 2010* (eds K. E. MacFarlane, L. H. Weston & C. Relf), pp. 161–82. Yukon Geological Survey.

Magnusson, N. H. 1960. Age determination of Swedish Precambrian rocks. *Geologisk Föreningens i Stockholm Förhandlingar* **82**, 407–32.

Martí Mus, M. & Moczydłowska, M. 2000. Internal morphology and taphonomic history of the Neoproterozoic vase-shaped microfossils from the Visingsö Group, Sweden. *Norsk Geologisk Tidsskrift* **80**, 213–28.

Milles, B., Watson, A. J., Goldblatt, C., Boyle, R. & Lenton, T. M. 2011. Timing of Neoproterozoic glaciations linked to transport-limited global weathering. *Nature Geoscience* **4**, 861–4.

Moczydłowska, M. 2008a. The Ediacaran microbiota and the survival of Snowball Earth conditions. *Precambrian Research* **167**, 1–15.

Moczydłowska, M. 2008b. New records of late Ediacaran microbiota from Poland. *Precambrian Research* **167**, 71–92.

Moczydłowska, M. 2016. Algal affinities of the Ediacaran and Cambrian organic-walled microfossils with internal reproductive bodies: *Tanarium* and other morphotypes. *Palynology* **40**, 83–121.

Moczydłowska, M., Landing, E., Zang, W. & Palacios, T. 2011. Proterozoic phytoplankton and timing of Chlorophyte algae origins. *Palaeontology* **54**, 721–33.

Moczydłowska, M. & Nagovitsin, K. 2012. Ediacaran radiation of organic-walled microbiota recorded in the Ura Formation, Patom Uplift, East Siberia. *Precambrian Research* **198–199**, 1–24.

Möller, C., Andersson, J., Dyck, B. & Lundin, I. 2015. Exhumation of an eclogite terrane as a hot migmatitic nappe, Sveconorwegian orogeny. *Lithos* **226**, 147–68.

Morad, S. & Al-Aasm, I. S. 1994. Conditions of formation and diagenetic evolution of Upper Proterozoic phosphate nodules from southern Sweden: evidence from petrology, mineral chemistry and isotopes. *Sedimentary Geology* **88**, 267–82.

Mukherjee, I. & Large, R. R. 2016. Pyrite trace element chemistry of the Velkerri Formation, Roper Group, McArthur Basin: evidence for atmospheric oxygenation during the Boring Billion. *Precambrian Research* **281**, 13–26.

Nagy, R. M., Porter, S. M., Dehler, C. M. & Shen, Y. 2009. Biotic turnover driven by eutrophication before the Sturtian low-latitude glaciation. *Nature Geoscience* **2**, 415–8.

Narbonne, G. M. 2005. The Ediacara biota: Neoproterozoic origin of animals and their ecosystems. *Annual Reviews of Earth and Planetary Sciences* **33**, 421–42.

Narbonne, G. M., Xiao, S. & Shields, G. A. 2012. The Ediacaran Period. In *The Geologic Time Scale 2012*, Vol. 1, (eds F. M. Gradstein, J. G. Ogg, M. D. Schmitz & G. M. Ogg), pp. 413–35. Amsterdam: Elsevier.

Ogurtsova, R. N. & Sergeev, V. N. 1989. Megaspheromorphids from the Upper Precambrian Chichkanskaya Formation, southern Kazakhstan. *Paleontologicheskii Zhurnal* **2**, 119–22 (in Russian).

Partin, C. A., Bekker, A., Planavsky, N. J., Scott, C. T., Gill, B. C., Li, C., Podkovyrov, V., Maslov, A., Konhauser, K. O., Lalonde, S. V., Love, G. D., Poulton, S. W. & Lyons, T. W. 2013. Large-scale fluctuations in Precambrian atmospheric and oceanic oxygen levels from the record of U in shale. *Earth and Planetary Sciences Letters* **369–370**, 284–93.

Pease, V., Daly, J. S., Elming, S.-Å., Kumpulainen, R., Moczydłowska, M., Puchkov, V., Roberts, D., Saintot, A. & Stephenson, R. 2008. Baltica in the Cryogenian, 850–630 Ma. *Precambrian Research* **160**, 46–65.

Planavsky, N. J., Reinhard, C. T., Wang, X., Thomson, D., Mcgoldrick, P., Rainbird, R. H., Johnson, T., Fischer, W. & Lyons, T. W. 2014. Low Mid-Proterozoic atmospheric oxygen levels and the delayed rise of animals. *Science* **346**, 635–8.

Planavsky, N. J., Tarhan, L. G., Bellefroid, E. J., Evans, D. A. D., Reinhard, C. T., Love, G. D. & Lyons, T. W. 2015. Late Proterozoic transitions in climate, oxygen, and tectonics, and the rise of complex life. In *Earth-Life Transitions: Paleobiology in the Context of Earth System Evolution*(eds P. D. Polly, J. J. Head & D. L. Fox), pp. 1–36. *The Paleontological Society Papers* **21**.

Porter, S. M. 2006. The Proterozoic fossil record of heterotrophic eukaryotes. In *Neoproterozoic Geobiology and Paleobiology* (eds S. Xiao & A. J. Kaufman), pp. 1–21. Dordrecht: Springer.

Porter, S. M. & Knoll, A. H. 2000. Testate amoebae in the Neoproterozoic Era: evidence from vase-shaped microfossils in Chuar Group, Grand Canyon. *Paleobiology* **26**, 360–85.

Porter, S. M., Meinsterfeld, R. & Knoll, A. H. 2003. Vase-shaped microfossils from the Neoproterozoic Chuar Group, Grand Canyon: a classification guided by modern testate amoebae. *Journal of Paleontology* **77**, 409–29.

Porter, S. M. & Riedman, L. A. 2016. Systematics of organic-walled microfossils from the ca. 780–740 Ma Chuar Group, Grand Canyon, Arizona. *Journal of Paleontology* **90**, 815–53.

Poulton, S. W. & Canfield, D. E. 2011. Ferruginous conditions: a dominant feature of the ocean through Earth's history. *Elements* **7**, 107–12.

Riedman, A. L., Porter, S. M., Halverson, G. P., Hurtgen, M. T. & Junium, C. K. 2014. Organic-walled microfossil assemblage from glacial and interglacial Neoproterozoic units of Australia and Svalbard. *Geology* **42**, 1011–14.

Sahoo, S. K., Planavsky, N. J., Jiang, G., Kendall, B., Owens, J. D., Wang, X., Shi, X., Anbar, A. D. & Lyons, T. W. 2016. Oceanic oxygenation events in the Ediacaran ocean. *Geobiology* **14**, 457–68.

Schirrmeister, B. E., Gugger, M. & Donoghue, P. C. J. 2015. Cyanobacteria and the Great Oxidation Event: evidence from genes and fossils. *Palaeontology* **58**, 769–85.

Schopf, J. W. 1992. Proterozoic Prokaryotes: affinities, geologic distribution, and evolutionary trends. In *The Proterozoic Biosphere A Multidisciplinary Study* (eds J. W. Schopf & C. Klein), pp. 195–218. New York: Cambridge University Press.

Sergeev, V. N. 2006. Precambrian microfossils on cherts: their paleobiology, classification and biostratigraphic usefulness. *Moscow, GEOS, Transactions of the Geological Institute* **567**, 1–280 (in Russian).

Sergeev, V. N., Knoll, A. H., Vorobeva, N. G. & Sergeeva, N. D. 2016. Microfossils from the lower Mesoproterozoic Kaltasy Formation, East European Platform. *Precambrian Research* **278**, 87–107.

Sergeev, V. N. & Schopf, J. W. 2010. Taxonomy, paleoecology and biostratigraphy of the Late Neoproterozoic Chichkan microbiota of South Kazakhstan: the marine biosphere on the eve of metazoan radiation. *Journal of Paleontology* **84**, 363–401.

Söderlund, U., Isachsen, C., Bylund, G., Heaman, L. M., Patchett, P. J., Vervoort, J. & Andersson, U. B. 2005. U–Pb baddeleyite ages and Hf, Nd isotope chemistry constraining repeated mafic magmatism in the Fennoscandian Shield from 1.6 to 0.9 Ga. *Contributions to Mineralogy and Petrology* **150**, 174–94.

Spence, G. H., Le Heron, D. L. & Fairchild, I. J. 2016. Sedimentological perspectives on climatic, atmospheric and environmental change in the Neoproterozoic Era. *Sedimentology* **63**, 253–306.

Sperling, E. A., Frieder, C. A., Raman, A. V., Girguis, P. R., Levin, L. A. & Knoll, A. H. 2013. Oxygen, ecology, and the Cambrian radiation of animals. *Proceedings of the National Academy of Sciences USA* **110**, 13446–51.

Stephens, M. B., Ripa, M., Lundström, I., Persson, L., Bergman, T., Ahl, M., Wahlgren, C. H., Persson, P. O. & Wickström, L. 2009. *Synthesis of the Bedrock Geology in the Bergslagen Region. Fennoscandian Shield, South-Central Sweden*. Sveriges geologiska undersökning (SGU) Report, Serie Ba 58, 259 pp.

Strauss, J. V., Rooney, A. D., Macdonald, F. A., Brandon, A. D. & Knoll, A. H. 2014. 740 Ma vase-shaped microfossils from Yukon, Canada: implications for Neoproterozoic chronology and biostratigraphy. *Geology* **42**, 659–62.

Swanson-Hysell, N. L., Maloof, A. C., Condon, D. J., Jenkin, G. R. T., Alene, M., Tremblay, M. M., Tesema, T., Rooney, A. D. & Haileab, B. 2015. Stratigraphy and geochronology of the Tambien Group, Ethiopia: evidence for globally synchronous carbon isotope change in the Neoproterozoic. *Geology* **43**, 323–6.

Tang, Q., Pang, K., Xiao, S., Yuan, X., Ou, Z. & Wan, B. 2013. Organic-walled microfossils from the early Neoproterozoic Liulaobei Formation in the Huinan region of North china and their biostratigraphic significance. *Precambrian Research* **236**, 157–81.

Tang, Q., Pang, K., Yuan, X., Wan, B. & Xiao, S. M. 2015. Organic-walled microfossils from the Tonian Gouhou Formation, Huaibei region, North China Craton, and

their biostratigraphic implications. *Precambrian Research* **266**, 296–318.

Tang, D., Shi, X., Wang, X. & Jiang, G. 2016. Extremely low oxygen concentration in mid-Proterozoic shallow seawaters. *Precambrian Research* **276**, 145–57.

Turner, E. C. & Bekker, A. 2016. Thick sulfate evaporate accumulations marking a mid-Neoproterozoic oxygenation event (Ten Stone Formation, Northwest Territories, Canada). *Geological Society of America Bulletin* **128**, 203–22.

Ulmius, J., Andersson, J. & Möller, C. 2015. Hallandian 1.45 Ga high-temperature metamorphism in Baltica: P–T evolution and SIMS U–Pb zircon ages of aluminous gneisses, SW Sweden. *Precambrian Research* **265**, 10–39.

Van Kranendonk, M. J., Altermann, W., Beard, B. L., Hoffmsan, P. F., Johnson, C. M., Kasting, J. F., Melezhik, V. A., Nuyman, A. P., Papineau, D. & Pirajno, F. 2012. A chronostratigraphic division of the Precambrian. In *The Geologic Time Scale 2012*, Vol. 1 (eds F. M. Gradstein, J. G. Ogg, M. D. Schmitz & G. M. Ogg), pp. 299–392. Amsterdam: Elsevier.

Vidal, G. 1972. Algal stromatolites from the Late Precambrian of Sweden. *Lethaia* **5**, 353–68.

Vidal, G. 1974. Late Precambrian microfossils from the basal sandstone unit of the Visingsö Beds, South Sweden. *Geologica et Palaeontologica* **8**, 1–14.

Vidal, G. 1976. Late Precambrian microfossils from the Visingsö Beds in southern Sweden. *Fossils and Strata* **9**, 1–57.

Vidal, G. 1979. Acritarchs from the Upper Proterozoic and Lower Cambrian of East Greenland. *Grønlands Geologiske Undersøgelse Bulletin* **134**, 1–40.

Vidal, G. 1982. Den prepaleozoiska sedimentära berggrunden. In *Description to the Map of Solid Rocks Hjo NO*, pp. 52–76. Sveriges geologiska undersökning, Serie Af 120.

Vidal, G. 1985. Prepaleozoisk sedimentberggrund. In *Beskrivning till Bergrundskartan Hju SO (Description to the Map of Solid Rocks Hju SO)* (eds L. Persson, Å. Brunn & G. Vidal), pp. 77–91. Sveriges geologiska undersökning, Serie Af 134.

Vidal, G. 1994. Early ecosystems: limitations imposed by the fossil record. In *Early Life on Earth* (ed. S. Bengtson), pp. 298–311. Nobel Symposium No. 84. New York: Columbia University Press.

Vidal, G. & Ford, T. 1985. Microbiotas from the late Proterozoic Chuar Group (northern Arizona) and Uinta Mountain Group (Utah) and their chronostratigraphic implications. *Precambrian Research* **28**, 349–489.

Vidal, G. & Moczydłowska, M. 1995. The Neoproterozoic of Baltica–stratigraphy, palaeobiology and general geologic evolution. *Precambrian Research* **73**, 197–216.

Vidal, G. & Moczydłowska-Vidal, M. 1997. Biodiversity, speciation, and extinction trends of Proterozoic and Cambrian phytoplankton. *Paleobiology* **23**, 230–46.

Viola, G., Henderson, I. H. C., Bingen, B. & Hendriks, B. W. H. 2011. The Grenvillian–Sveconorwegian orogeny in Fennoscandia: back-thrusting and extensional shearing along the "Mylonite Zone". *Precambrian Research* **189**, 368–88.

Xiao, S., Shen, B., Tang, Q., Kaufman, A. J., Yuan, X., Li, J. & Qian, M. 2014a. Biostratigraphic and chemostratigraphic constraints on the age of early Neoproterozoic carbonate successions in North China. *Precambrian Research* **246**, 208–25.

Xiao, S., Zhou, C., Liu, P., Wang, D. & Yuan, X. 2014b. Phosphatized acanthomorphic acritarchs and related microfossils from the Ediacaran Doushantuo Formation at Weng'an (South China) and their implications for biostratigraphic correlation. *Journal of Paleontology* **88**, 1–67.

Yan, Y. & Liu, Z. 1993. Significance of eukaryotic organisms in the microfossil flora of Changcheng System. *Acta Micropalaeontologica Sinica* **10**, 167–80.

Ye, Q., Tong, J., Xiao, S., Zhu, S., An, Z., Tian, L. & Hu, J. 2015. The survival of benthic macroscopic phototrophs on a Neoproterozoic Snowball Earth. *Geology* **43**, 507–10.

Zhang, W., Roberts, D. & Pease, V. 2015. Provenance characteristics and regional implications of Neoproterozoic, Timanian-margin successions and a basal Caledonian nappe in northern Norway. *Precambrian Research* **268**, 153–67.

Zhang, S., Wang, X., Wang, H., Bjerrum, C. J., Hammarlund, E. U., Costa, M. M., Connelly, J. N., Zhang, B., Su, J. & Canfield, D. E. 2016. Sufficient oxygen for animal respiration 1,400 million years ago. *Proceedings of the National Academy of Sciences USA* **113**, 1731–6.